Published in final edited form as:
Magn Reson Med. 2009 May ; 61(5): 1073–1082. doi:10.1002/mrm.21857.

Direct MRI Mapping of Neuronal Activity Evoked by Electrical Stimulation of the Median Nerve at the Right Wrist

Yiqun Xue[1,2], **Xiying Chen**[2], **Thomas Grabowski**[3], and **Jinhu Xiong**[2]

[1]Department of Biomedical Engineering, University of Iowa, Iowa City, IA, 52240

[2]Department of Radiology, University of Iowa, Iowa City, IA, 52240

[3]Department of Neurology, University of Iowa, Iowa City, IA, 52240

Abstract

Magnetic source MRI (msMRI) has being developed recently for direct detections of neuronal magnetic fields to map brain activity. However, controversial results have been reported by different research groups. In this paper, more evidence was provided to demonstrate that the neuronal current signal could be detected by MRI using a rapid median nerve stimulation paradigm. The experiments were performed on six normal human participants to investigate the temporal specificity of the effect, as well as inter- and intra-subject reproducibility. Significant activation of contra-lateral primary sensory cortex (S1) was detected 80ms after stimulation onset (corresponding to the P80 evoked potential peak). The 80 ms latency S1 activation was observed over 3 independent sessions for one subject and for all 6 participants. The magnitude of the signal change was 0.2% - 0.3%. Coinciding with our expectations, no S1 activation was found when MRI data acquisitions were targeted at the N20 and P30 peaks because of mutual cancellation of magnetic fields generated by those peaks. The results demonstrated good reproducibility of S1 activations and indicated that the S1 activations most likely originated from neuronal magnetic field rather than hemodynamic response.

Keywords

Magnetic source MRI; Direct neuronal detection; Neuronal magnetic field; fMRI

Introduction

Direct detections of transient neuronal magnetic fields using MRI offer several advantages over the conventional functional MRI (fMRI) techniques, which measure regional cerebral hemodynamic response induced by neural firing (1-4). Because it directly measures the effects of neuronal magnetic fields, the novel fMRI technique, termed here as magnetic source MRI (msMRI), could avoid the assumption of close coupling of regional cerebral hemodynamics and neuronal activity. It can potentially offer higher temporal resolution and better spatial localization. The feasibility of msMRI has been studied theoretically and experimentally by several research groups (5-25). Controversial results have been reported. It is currently still a matter of debate whether the technique is practical for mapping neuronal activity.

Correspondence to: Jinhu Xiong.

Corresponding Author: Jinhu Xiong, Ph.D. Department of Radiology University of Iowa #3891 JPP, 200 Hawkins Drive Iowa City, Iowa 52242 Tel: 319-356-1183 Fax: 319-356-2220 E-mail address: jinhu-xiong@uiowa.edu.

The feasibility of directly mapping neuronal activity has been addressed theoretically. Divergent conclusions were reached by investigators considering different dipole models or measuring different parameters (i.e. phase and magnitude imaging). Initially, Singh (5) used an electrical current phantom to investigate the possibility of detecting the evoked neuromagnetic field. The neuronal magnetic field inside the brain was calculated on the basis of the field observed on the surface of the skull. It was reported that the required measurement of phase shifts was twenty-fold smaller than the sensitivity of the scanner they used. However, it is possible that the local neuronal magnetic field is much larger than they predicted since opposite neuronal currents have a cancellation effect which results in a much smaller field on the skull. Konn et al. (6) modeled neuronal current flow as an extended current dipole located in a conducting sphere. They demonstrated that the minimum detectable dipole strength by nuclear magnetic resonance under normal experimental conditions was similar in magnitude to dipole strengths from evoked neuronal activity. Further, it has been reported by Konn et al. (6) and Bodurka et al. (7) that phase imaging is a better approach than magnitude imaging based on the extended current dipole model. Xue et al. (8) presented a theoretical model which modeled each dendrite as a finite size dipole and considered contributions from all dendrites located in a typical MRI voxel. They concluded that the magnitude change of MRI signal is much more significant than phase change of the signal on a voxel scale, theoretically reaching magnitudes of as much as 2%. Pell et al. (9) further optimized MR sensitivity to transient and weak currents and suggested that it should be possible to detect current in nerves using magnitude imaging. Blagoev et al. (10) and Cassara et al. (11) presented more realistic models to simulate neuronal activities of single and multiple neurons. Both of them modeled the spatiotemporal distributions of the neuronal magnetic field. They concluded that MR signal changes were in the detectable range but depend highly on neuronal morphology and physiology properties.

Experimental results have also been reported by several other labs. Early phantom tests (7,12,13) showed that it is possible to detect the magnetic fields of the order of 10^{-10} T, which is similar to the magnitude of the magnetic field induced by neuron firing (26,27). The feasibility of direct detection of neuronal magnetic field has also been explored in human subject experiments. Kamei et al. (14) initially applied this technique to obtain maps of human brain activity by using motor and sensory stimulation paradigms. It was suggested that neuronal current induced MRI signal changes are dependent on the polarity of field gradient but other causes (i.e. susceptibility effect) are not, and that neuronal current effects could therefore be acquired by subtracting functional images acquired with opposite field gradients. Song and Takahashi (15), Truong and Song (16) demonstrated that a small neuronal current could be directly detected using MRI by measuring small spatial displacements induced by the Lorentz force on the conducting materials. In 2003, Xiong et al. (17) reported that neuronal activity in a visuomotor paradigm could be detected using gradient echo (GE) EPI sequence with a high temporal resolution (100 ms). Bianciardi et al. (18) subsequently presented preliminary results showing detection of a neuronal magnetic field effect using a spin echo (SE) MRI sequence. Liston et al. (19) reported a successful MRI detection of activations associated with generalized spike-wave discharges in a patient with epilepsy. Chow et al. (20,21) directly detected spectral components of the magnetic fields of ionic currents caused by the firing of optic nerve axons in response to visual strobe stimulation and reported a higher detectability for magnitude imaging than phase imaging. Petridou et al. (22) used organotypic rat-brain cultures *in vitro* and demonstrated that spontaneous neuronal activity could be detected directly using MRI in the absence of a cerebrovascular system. Several negative results have also been published. A notable result was reported by Chu et al. (23), who used a clever embedded binary m-sequence probe method to detect the neuron activity in the visual cortex. They reported the absence of any rapid phase or magnitude changes in this experiment. Similarly, Parkes et al. (24) presented a visual stimulation paradigm with random intervals to minimize the prediction effects.

Their results showed no activity that could be attributed to the neuromagnetic signals. Tang et al. (25) reported failure to detect the signal changes which were temporally correlated with the timings of evoked response potentials by using a hybrid ms/BOLD event related design.

In this paper, we will present a rapid median nerve stimulation paradigm and map brain activities in the contralateral primary somatosensory cortex (SI). We will investigate the temporal specificity of msMRI signals and demonstrate high temporal resolution of msMRI technique. We will also assess inter- and intra-subject reproducibility of our msMRI signals. Finally, we will discuss the optimal TE for detecting transient and weak neuronal magnetic fields.

Theory

msMRI Signal

A neuron typically consists of a single axon and tens to thousands dendrites. If each axon and dendrite is modeled as a current dipole, the magnetic field at any observation point P outside a neuron can be calculated according to the Biot-Savart law. The component of neuronal magnetic field, B_n, parallel to the B_0 (of the MRI scanner) will cause the spins at a point (x, y, z) in the transverse plane to acquire additional phases, $\varphi_1(x, y, z)$. The majority of $B_{n\perp}$, which is the component of the neuronal magnetic field perpendicular to the B_0, will have no net effect on the spins. Only a small fraction of $B_{n\perp}$ at the Larmor frequency will act like a B_1 field to rotate the spins at a point (x, y, z) away from the x -y plane. The fraction is typically very small. The effect of $B_{n\perp}$, therefore, can be ignored (8). Note that msMRI measures the integration of dephasing effect induced by neuronal magnetic field during TE. All activated neurons during TE contribute to the dephasing effect. This is different from MEG which measures the superposition of the neuronal magnetic field outside brain at a particular time. The MRI signal for an image voxel is an integral of MRI signal observed at any points (x, y, z) over the voxel:

$$S = \int_0^{\Delta x}\int_0^{\Delta y}\int_0^{\Delta z} \rho(x,y,z)\, e^{i\varphi_1(x,y,z)}\, dx\,dy\,dz, \quad [1]$$

where Δx, Δy, and Δz are the dimensions of the voxel, $\rho(x, y, z)$ is spin density. The magnitude of MRI signal is vector sum of all spins in the voxel. Since the additional phase can be positive or negative, the vector in the direction which is perpendicular to the rotating frame of reference will cancel each other out and can be ignored. The magnitude of MRI signal in the rotating frame of reference, therefore, is decreased by a factor of $\cos(\varphi_1(x, y, z))$ and the magnitude change can be written as:

$$\Delta S_m = \int_0^{\Delta x}\int_0^{\Delta y}\int_0^{\Delta z} \rho(x,y,z)\,(1-\cos(\varphi_1(x,y,z)))\, dx\,dy\,dz. \quad [2]$$

Since the additional phase shift $\varphi_1(x, y, z)$ is pretty small and very close to 0, according to the Taylor expansion, Eq. [2] can be rewritten as

$$\Delta S_m \approx \int_0^{\Delta x}\int_0^{\Delta y}\int_0^{\Delta z} \rho(x,y,z)\,\frac{\varphi_1(x,y,z)^2}{2}\, dx\,dy\,dz. \quad [3]$$

The magnitude change of MRI signal is roughly relative to the square of phase shift induced by the neuronal magnetic field. More details regarding field distribution, orientation and

temporal dynamics of the neuronal magnetic field have been discussed in the previous theoretical paper (8).

Optimal TE

For BOLD fMRI, the percentage signal change has a linear relation with TE and the contrast to noise ratio (CNR) is known to be optimized when TE=T2*. However, msMRI measures the accumulated dephasing effects of neuronal activity during the entire TE, msMRI signal should be stronger if a longer TE is used. Assuming these fired neurons are uniformly distributed within TE, the additional phase shift induced by neuronal magnetic field is linear to the length of TE. Based on Eq. [3], this relationship leads to

$$\Delta S_m \propto TE^2. \quad [4]$$

By taking into account the effect of T2* decay of spins and assuming noise is constant, the CNR is related to

$$CNR_m \propto SNR * \frac{\Delta S_m}{S_0} \cdot e^{-\frac{TE}{T_{2^*}}} \propto TE^2 \cdot e^{-\frac{TE}{T_{2^*}}} \quad [5]$$

It can be concluded that the maximal CNR happens when TE equals twice T2*. The T2* value varies with brain area and also highly depends on shimming. For grey matter, which is the tissue compartment we are interested in, the commonly used T2* for gray matter at 3T scanner is 40ms (28). The optimized TE is 80 ms. The real distribution of fired neuron is not uniform. The majority of neuron fired in a limited duration. So the additional phase shift is no longer linear to the length of TE. The optimal TE, therefore, should be less than twice T2*.

Methods

Subjects

Six healthy subjects (two men and four women, aged 25-32) participated in this study. All subjects were right handed. Informed consent in accordance with local and federal standards was obtained from each participant prior to the study. Subjects lay supine inside the magnet bore throughout the experiment during the presentation of electrical stimuli. Head movement was minimized by mild restraint and cushioning.

Paradigm

Unilateral stimulations were delivered to the median nerve at the right wrist by a Grass S8 stimulator. The electrical noise from the stimulator is not significant based on our phantom and human test. The electric stimulus was a square wave pulse with a duration of 0.2 msec. The shock intensity was adjusted to obtain a thumb twitch. Pulse amplitudes ranged from 80-120 V. Subjects were asked not to actively perform any task, but to keep still and awake. By only detecting the passive neuron response to the electrical stimulation, variances in response timing due to subject motivation and attention have been minimized. Because msMRI directly detects neuronal response and has high temporal resolution, reducing uncertainties in stimulus timing can greatly enhance the sensitivity for msMRI signals that occur in a narrow temporal window.

Unilateral stimulation of median nerve activates the contralateral primary somatosensory cortex (SI). A series of somatosensory evoked potentials (SEPs) (i.e. N20-P30-N45-P80) in

area SI have been reported by Allison et al. (29,30) who directly recorded SEPs from the exposed cortical surface. The timing information, therefore, directly reflects the neuron activity in the cortex (29,30) To investigate temporal properties of msMRI signals, we targeted our data acquisitions at different components of the SEPs (N20/P30 and P80). The earliest cortical response peaks at 20ms after median nerve stimulation. This negative peak (N20) originates at area 3b of the SI cortex. In other words, the direction of the intracellular current is from the deep layer towards the superficial layer of area 3b of the SI cortex, consistent with excitation in the deep cortical layers. The next deflection has the opposite polarity and peaks at 30-35 ms (P30) after stimulation. This P30 response most probably reflects net intracellular current from surface to depth in the SI cortex. The late potential, P80, was reported by Allison et al. (29) and this component localizes to Brodmann area 2 (BA2).

There are several advantages for the rapid median nerve stimulation design over previous designs. The stimulus onset asynchrony (SOA) and timing of the neuronal response could be accurately controlled. Moreover, the BOLD effect was minimized by the design. Different SOAs were used to detect the different response components and demonstrate the temporal specificity of msMRI effects.

Protocol and Data acquisitions

All MRI data were acquired at Siemens 3.0 T Trio scanner (Siemens Medical Solutions, Erlangen, Germany). T1-weighted anatomical images were acquired to facilitate the precise determination of the brain structures. The parameters for T1-weighted images were: TR=1590 ms, TE=2.48 ms, flip angle=10 degrees, voxel size=0.86 × 0.86 × 6 mm^3. Both BOLD imaging and msMRI imaging were performed on each subject. BOLD imaging was performed first to identify activated brain regions. Sixteen slices were selected and a conventional block design was used with three 40 sec off-on cycles. The stimuli were delivered every two seconds during the task block. A gradient echo EPI pulse sequence was used with imaging parameters: TR=2000 ms, TE=40 ms, flip angle=80 degree, in-plane resolution 3×3 mm^2 and slice thickness 5 mm with 1 mm gap. Activation maps were calculated immediately after the scan by using an online t-test analysis.

In the msMRI phase of the experiment, a gradient echo EPI pulse sequence was used with TR/TE/flip angle parameters of 300 ms/60 ms/40 degree. An inter-stimulus-interval (ISI) of 600 ms was used to drive the BOLD MRI signal to steady state. Each run included 600 stimulation ON/OFF cycles with two images for each cycle (one ISI). Stimulus delivery was synchronized with the trigger signal from MRI scanner to provide accurate control on timing. Three contiguous slices were scanned with ascending order. The middle slice was targeted on the subjects' S1 area. In this experiment, we were concerned to detect the dephasing effect of neuronal magnetic field in this area. Three different SOAs were used in our msMRI experiments. Figure 1a shows the timing for detecting msMRI activation at 80ms latency. Data was acquired from 50 ms to 110 ms after stimulation onset so that the 80 ms latency component completely fell into TE. Figure 1b shows the timing for detecting the early components (0~60 ms). In Figure 1c, the electrical stimuli (100 ms after the trigger from scanner) were delivered after the target slice was scanned. For this case, the data from the target slice should not contain any neuronal current effects induced by stimulation. Control scans in which no stimulation was applied were also performed for every subject.

Data analysis

The MRI images were processed in the MATLAB environment (MathWorks Inc., Natick, MA, USA). The first 40 images of each run were discarded to allow hemodynamics and MRI signal to reach a steady state. A two-dimensional (2-D) motion correction was carried

out to minimize in-plane motion. Data interpolation between image slices was purposely avoided because different slices were acquired at different times. Voxel-by-voxel linear detrending was used to remove the linear drift of the MRI signal. The heartbeat rate and respiration rate of the subject were measured before each scan and a proper temporal high pass filter was then applied to remove the respiration frequency and the aliased frequency of the heartbeat. A mean image was created for each off-on cycle by averaging the time-series in the cycle, and then subtracted from each image to create residual images. A 2-D spatial Gaussian filter with a full width at half magnitude (FWHM) of 4.5 mm was applied. A group student's *t*-test was then performed on the residual images. The *t* map was then thresholded using an intensity threshold of 3.0 ($P < 0.0013$) and cluster size threshold of two voxels to detect significant activation assuming the msMRI activation extended several mm^2.

Results

Figure 2 shows BOLD activation maps for two contiguous slices which cover primary sensory cortex (S1). Activations were found in contralateral S1 (close to BA2), primary motor cortex (M1) and the supplementary motor area (SMA). These results are consistent with previous fMRI studies conducted with similar electrical stimulation (31,32).

To assess the consistency of msMRI signal across different scan sessions, msMRI experiments were performed on one of the subjects in three different scanning days. The activation maps for the 80ms latency component and for the control scans are shown in Figure 3. Significant activations were found close to Brodmann areas 2 (BA 2) for all three 80ms latency scans (Figure 3a-3c). Since the 80ms latency component is the late response of median nerve stimulation, the locations of the activations are closer to the anterior wall of the postcentral sulcus (BA 2), rather than the posterior wall of the central sulcus (area 3b) where the early components (N20, P30) were expected. Our results are consistent with the location of P80 potential reported by Allison et al. (29). Activations were also found in some other areas (i.e. M1) but not consistent over all scans. Control scans in which no stimuli were applied were also performed for each session. As expected, the activation maps for the control scans (Figure 3d-3f) are much cleaner than the 80ms latency activation maps. Specifically, no control scan demonstrated activation in the S1 area.

Time-course plots corresponding to the activated area and the non-activated area in 80ms latency scans are shown in Figure 4. Each point on the time course was calculated by averaging 120 images. There is a significant magnitude change between baseline and activation in the activated S1 area. The mean magnitude of signal change was 0.24%. Our result is similar to the finding reported by Chow et al. (20), who demonstrated a 0.15% perturbation of baseline signal in their experiment. To estimate the MRI signal change induced by fluctuation of BOLD signal, a theoretical calculation was performed to simulate BOLD effect using Gamma variate function. We assume that the magnitude of event related BOLD signal is 1.5% and ISI is 600 ms. To simulate the nonlinear relationship between the neuronal activation and BOLD response, we used 100ms jitter to simulate the time variance of BOLD response. We also considered the magnitude of BOLD response with 20% random change. The maximal MRI signal variation due to the fluctuation of BOLD signal is less than 0.05%, which is much smaller than the msMRI signal we measured and can be safely ignored.

Identical experiments were performed on six individual subjects to assess the reproducibility of msMRI results with this paradigm across different subjects. msMRI activation maps for the 80ms latency component for these subjects are shown in Figure 5. All subjects demonstrate an S1 response in the vicinity of the posterior wall of the post central sulcus. By

contrast, activations in other brain areas were not as reproducible. This inconsistency might relate to less direct temporal connection of these responses to stimulation times, or to differences in slice positions and orientations across different subjects.

Different stimulus onset asynchronies were used to explore the timing effect of msMRI. As Figure 1b and 1c show, the onsets of stimuli were adjusted to acquire the activation maps induced by different components. Figure 1b shows the timing for measuring dephasing effects of early components (0~60ms). Since there are several SEPs with opposite orientations during this time, the overall dephasing effect of these SEPs are weakened by a cancellation effect. Our result (Figure 6b) demonstrated no significant activation in the S1 area, which agrees well with our expectation. Figure 1c shows the paradigm in which the images were acquired before stimulation. No msMRI effect was anticipated in this scan. As expected, the activation maps (Figure 6c) are much cleaner than the 80ms latency activation maps. We found no activation in S1 area.

To demonstrate the TE dependence of msMRI, additional scans for TE=30, 60 and 80ms were conducted. All experiments were performed on a single subject (Subject 6) on the same day. The timing of stimulation onset was adjusted so that the center of TE (TE/2) was always located at 80ms after stimulus. Data was processed for each individual TE to generate three activation maps (one for each TE). A ROI was defined by combining all activated voxels in the S1 area of the three activation maps. Figure 7 shows the activation maps for three different TEs. We found significant activation in S1 area for both TE of 30 ms and 60 ms, but no activation in S1 area for TE of 80 ms. The signal percentage changes in the ROI for TE =30, 60, 80 ms are 0.15%, 0.26%, 0.25% respectively. While the signal percentage change for TE of 80 ms was close to TE of 60 ms, the CNR for TE of 80 ms was only 57% of the CNR for TE of 60 ms by taking into account the T2* decay. This may explain why no activation is detected for TE = 80 ms. Figure 8 shows the simulated and experimental signal percentage changes for different TEs and different distributions (uniform and normal distributions). For the normal distribution, the peak is located at 80ms after the stimulation onset and the variance is 225 (N(80, 225)). The neuronal magnetic fields and signal percentage changes were calculated based on our previous theoretical modeling paper (8). Since the duration of neural firing was limited (60 ms), the maximal signal percentage change was happened when TE=60 ms. The measured signal percentage changes were between the simulated signal percentage changes for uniform distribution and normal distribution. Based on our calculation, the optimized TE is around 40ms for the normal distribution and is 80ms for the uniform distribution. Therefore, we believe that the optimal TE for detecting the dephasing effect induced by P80 component should be between 40 and 80ms (A TE of 60 ms was used in our experiments).

DISCUSSION AND CONCLUSION

In this work, we present a rapid median nerve stimulation paradigm for the detection of msMRI signal. Our initial results are demonstrating a consistent 80 ms latency activation of the primary somatosensory cortex, within subject and across subjects. Earlier components were not detected, consistent with the expected cancellation effect of bi-polar neuronal magnetic fields. As expected, the magnitude of the msMRI signal was 0.2%~0.3%.

1. Consistency

As our results indicate, msMRI contrast is much weaker than BOLD contrast. Despite the small magnitude of the signal, it is consistently present. In subject 1, S1 activation was demonstrable in each of three sessions, conducted on different scanning days (Figure 3). Significant activations were found in S1 and M1 areas in 80ms latency scans. No such activations were seen in these areas in the control scans on each date. The result was also

consistent across subjects. S1 was activated in each of the six individuals, implicating a sector of the anterior wall of the postcentral sulcus (Figure 5). Activations in other brain areas were not very consistent across different subjects and different sessions for the same subjects. Possible reasons for such inconsistency include: 1) Variations in slice incidence and location. In our experiments, the slice positions were manually selected for each repeat scans to cover the S1 areas. We paid a little attention to other brain areas. Slice orientations and positions may change from scan to scan. The activations in other areas will be missed if they are not in the same slice. The variations in slice orientations and potions will increase the inconsistent in activation. 2) The temporal TE window we selected in our experiment was optimized to detect the activity in area S1. The activities in other brain areas may have different onset and offset times and may have different waveforms. This will increase variability of brain activation, even for the scans acquired for the same subject with different timing. 3) The responses in other areas may have a larger variance in both timing and magnitude across subjects. For example, even though the activations in SMA can be clearly identified in BOLD results, it has been reported that no ERPs can be detected in this area (33). 4) Those activations could also be induced by random noise, motion and, physiology artifacts. We could not completely rule out this possibility.

2. Timing effect

msMRI is a technique with high temporal resolution. It is thus quite sensitive to the onset and offset of stimulus. Different components of neuronal responses are measured by using different SOAs. In our experiments, three different SOAs (-50 ms, 0 ms and 100 ms relative to the trigger from scanner) were used in msMRI scans to measure the dephasing effect of different components. Our results demonstrated that neural responses with different latencies had different dephasing effects. The 80 ms latency component is a relatively long response that doesn't change orientation (sign) during TE. The overall msMRI contrast, therefore, will be maximized since msMRI measured an accumulated dephasing effect during TE. In contrast, early components (0~60 ms) include several SEPs with opposite orientations (signs) that are spatially proximate to each other, e.g. in adjacent banks of the central sulcus. The dephasing effects will be canceled out and make these components undetectable. This notion is consistent with our results (Figure 6b). When the target slice was acquired 100ms before the stimuli were applied, no dephasing effect was anticipated. As expected, there are no activations found in S1 area (Figure 6c). Bianciardi (18) reported similar temporal property. They used spin echo sequence to reverse the dephasing effect from the opposite neuronal magnetic fields and minimized the cancellation effect. In short, gradient echo sequence is suitable to detect the neuronal current effect without sign change. In contrast, spin echo sequence may be a good choice for neuronal magnetic field with sign change. The timing property supports our claim that the activations we detected were most likely from neuronal current effects rather than hemodynamic response.

3. msMRI vs. BOLD contrast

Neuronal activity induces not only neuronal magnetic field, but also a change of blood flow or blood oxygenation level. Thus it needs to be discussed whether our activations were actually due to msMRI contrast or perhaps to BOLD effect or noise. We believe the results we reported are indeed msMRI effects, for the following reasons. 1) In this study, we used a high stimuli presentation rate to drive the BOLD response to steady state. BOLD response was saturated in the steady state in this case. All the data were acquired during this steady state phase. Further, each trial consists of one activation image and one control image. The activation state is directly compared to the control state. Any signals common for both the control and the activation images were removed. Since each trial was acquired with very short interval (600 ms), the slowly changing BOLD effect and other physiological noises were better suppressed. The BOLD contribution is less than 0.05%, based on our

simulations. The signal from neuronal currents, therefore, should be the dominant signal. 2) msMRI has a high temporal resolution and is very sensitive to the timing of stimulation. Different SOAs may generate complete different results. The BOLD response, however, is slow and long lasting, and much less sensitive to the SOAs. In addition, BOLD contrast has no such cancellation effect since the blood oxygenation level always increases when neurons are activated. Therefore, the strong SOA dependence of our results strongly suggests that the activations we found were induced by neuronal magnetic fields rather than BOLD effects.

A long ISI design was also performed for this study. A pretty long ISI (19.8 sec) was used to allow the BOLD signal return to baseline. Most contribution from the BOLD effect was eliminated. However, this design is not very time efficient. Only 18 pairs (18 controls and 18 activations) of data were collected in a 6-min long scan. No significant activation was found in S1 area. The reason, we believe, is that the SNR is not high enough for detecting neuronal signals. For comparison, we collected 600 pairs of data in our short ISI design. It would take an extremely long scan session (hours) to achieve a similar SNR for the long ISI design. Similar discussion and conclusion have been presented in Hagberg et al's paper (34).

4. Optimal TE

As we stated in the method section, TE selection depends on 1) T2* values 2) duration and shape of the neuronal magnetic field. For an infinitely long and uniformly distributed activation, the optimal TE is two times T2* of the tissue. When the duration of activation is limited and the shape of neuronal magnetic field is not uniformly distributed, the optimal TE is less than two times T2*. In this study, the P80 component lasts about 60ms (29). A long TE (>60ms) would not increase signal percentage change but result in a lower CNR. The signal percentage change for TE=80 ms was 0.25% which was similar to the signal percentage change for TE=60 ms (0.26%). However, the CNR for TE of 80 ms was only 57% of the CNR for TE of 60 ms by taking into account the T2* decay. Moreover, the real distribution of fired neurons were not uniformly distributed during TE. The majority of neuron fired around 80 ms after the onset of stimulation. Our results (Figure 8) demonstrated that the optimal TE for detecting the dephasing effect induced by P80 component should be between 40 ms and 80 ms. The TE of 60 ms we used in this experiment should be good selection while it may not be a optimal value. More detailed studies are needed to clarify this issue.

5. msMRI CNR

A previous MEG study (33) has reported that the evoked magnetic fields on the scalp (2-4 cm away from the current source) are on the order of $\Delta B=10^{-13}$ T. It could be assumed that at least 50,000 or more cortical neurons that occupy an area of a few mm^2 must fire simultaneously and coherently to generate such a field strength (26,35). Since msMRI measures the accumulated effect of neuronal magnetic field, the overall signal changes induced by neuronal magnetic field during TE (60 ms used in this study) could be 0~0.7% based on the model of Xue et al. (8). It should be noted that 0.7% is the signal change for the extreme situation (all dipoles are in the same direction). For real application, the signal change should be smaller than 0.7%. From our experiment results, we found a 0.2%~0.3% signal change, which is in the range of the signal change predicted above.

To increase CNR, a total of 1200 images, 5-10 times more than conventional BOLD fMRI, were acquired to improve the statistic power. By taking account of the lower magnitude of msMRI signal and lower flip angle we used in this experiment, the overall CNR is about five times lower than BOLD imaging. Nevertheless, it is still possible for current MRI techniques to detect the activation. Besides system noise, some other sources of noise could also potentially lower the CNR and decrease msMRI signal detectability. Physiological

noise, such as heartbeat (1.1-1.4 Hz) and respiration (0.15-0.25 Hz), is significant for experiments aiming at detecting neuronal currents by MRI. Our simulation rate was chosen as 1.67 Hz to avoid these physiological frequencies. A temporal high pass filter was applied to minimize the physiological noises. In addition, since each slice was acquired at a different time, any interpolations between the slices could be avoided. CNR, therefore, will suffer from the movement of the subjects, especially in longitude direction.

In summary, this study shows a transient and weak, but consistent task-induced msMRI signal detected in S1 by msMRI. The magnitude change of MRI signal was around 0.2~0.3%. The intrinsic temporal sensitivity of msMRI technique is demonstrated. This temporal sensitivity must be respected in experimental design. While we demonstrated msMRI signal is in the detectable range of current fMRI technique, CNR is still much lower than BOLD imaging. Further work is required to improve experiment design and CNR to confirm our findings.

Acknowledgments

This work is financially supported by NSF (BCS 05-09626) and NIH (5 RO1 NS046082) grants. We would like to thank Peter J. Seaba for his technical assistance.

REFERENCES

1. Belliveau JW, Kennedy DN Jr, McKinstry RC, Buchbinder BR, Weisskoff RM, Cohen MS, Vevea JM, Brady TJ, Rosen BR. Functional mapping of the human visual cortex by magnetic resonance imaging. Science. 1991; 254:716–719. [PubMed: 1948051]
2. Bandettini PA, Wong EC, Hinks RS, Tikofsky RS, Hyde JS. Time course EPI of human brain function during task activation. Magn Reson Med. 1992; 25:390–397. [PubMed: 1614324]
3. Kwong KK, Belliveau JW, Chesler DA, Goldberg IE, Weisskoff RM, Poncelet BP, Kennedy DN, Hoppel BE, Cohen MS, Turner R, et al. Dynamic magnetic resonance imaging of human brain activity during primary sensory stimulation. Proc Natl Acad Sci U S A. 1992; 89:5675–5679. [PubMed: 1608978]
4. Ogawa S, Tank DW, Menon R, Ellermann JM, Kim SG, Merkle H, Ugurbil K. Intrinsic signal changes accompanying sensory stimulation: functional brain mapping with magnetic resonance imaging. Proc Natl Acad Sci U S A. 1992; 89:5951–5955. [PubMed: 1631079]
5. Singh M. Sensitivity of MR phase shift to detect evoked neuromagnetic fields inside the head. IEEE Trans Nucl Sci. 1994; 41:349–351.
6. Konn D, Gowland P, Bowtell R. MRI detection of weak magnetic fields due to an extended current dipole in a conducting sphere: a model for direct detection of neuronal currents in the brain. Magn Reson Med. 2003; 50:40–49. [PubMed: 12815677]
7. Bodurka J, Bandettini PA. Toward direct mapping of neuronal activity: MRI detection of ultraweak, transient magnetic field changes. Magn Reson Med. 2002; 47:1052–1058. [PubMed: 12111950]
8. Xue Y, Gao JH, Xiong J. Direct MRI detection of neuronal magnetic fields in the brain: theoretical modeling. Neuroimage. 2006; 31:550–559. [PubMed: 16504542]
9. Pell GS, Abbott DF, Fleming SW, Prichard JW, Jackson GD. Further steps toward direct magnetic resonance (MR) imaging detection of neural action currents: Optimization of MR sensitivity to transient and weak currents in a conductor. Magn Reson Med. 2006; 55:1038–1046. [PubMed: 16602069]
10. Blagoev KB, Mihaila B, Travis BJ, Alexandrov LB, Bishop AR, Ranken D, Posse S, Gasparovic C, Mayer A, Aine CJ, Ulbert I, Morita M, Muller W, Connor J, Halgren E. Modelling the magnetic signature of neuronal tissue. NeuroImage. 2007; 37:137–148. [PubMed: 17544300]
11. Cassara AM, Hagberg GE, Bianciardi M, Migliore M, Maraviglia B. Realistic simulations of neuronal activity: A contribution to the debate on direct detection of neuronal currents by MRI. NeuroImage. 2008; 39:87–106. [PubMed: 17936018]

12. Scott GC, Joy ML, Armstrong RL, Henkelman RM. RF current density imaging in homogeneous media. Magn Reson Med. 1992; 28:186–201. [PubMed: 1461122]
13. Bodurka J, Jesmanowicz A, Hyde JS, Xu H, Estkowski L, Li SJ. Current-induced magnetic resonance phase imaging. J Magn Reson. 1999; 137:265–271. [PubMed: 10053158]
14. Kamei H, Iramina K, Yoshikawa K, Ueno S. Neuronal Current Distribution Imaging Using Magnetic Resonance. IEEE Trans Magn. 1999; 35:4109–4111.
15. Song AW, Takahashi AM. Lorentz effect imaging. Magn Reson Imaging. 2001; 19:763–767. [PubMed: 11551715]
16. Truong TK, Song AW. Finding neuroelectric activity under magnetic-field oscillations (NAMO) with magnetic resonance imaging in vivo. Proc Natl Acad Sci U S A. 2006; 103:12598–12601. [PubMed: 16894177]
17. Xiong J, Fox PT, Gao JH. Directly mapping magnetic field effects of neuronal activity by magnetic resonance imaging. Human Brain Mapp. 2003; 20:41–49.
18. Bianciardi M, Di Russo F, Aprile T, Maraviglia B, Hagberg GE. Combination of BOLD-fMRI and VEP recordings for spin-echo MRI detection of primary magnetic effects caused by neuronal currents. Magn Reson Imaging. 2004; 22:1429–1440. [PubMed: 15707792]
19. Liston AD, Salek-Haddadi A, Kiebel SJ, Hamandi K, Turner R, Lemieux L. The MR detection of neuronal depolarization during 3-Hz spike-and-wave complexes in generalized epilepsy. Magn Reson Imaging. 2004; 22:1441–1444. [PubMed: 15707793]
20. Chow LS, Cook GG, Whitby E, Paley MN. Investigating direct detection of axon firing in the adult human optic nerve using MRI. Neuroimage. 2006; 30:835–846. [PubMed: 16376108]
21. Chow LS, Cook GG, Whitby E, Paley MN. Investigation of MR signal modulation due to magnetic fields from neuronal currents in the adult human optic nerve and visual cortex. Magn Reson Imaging. 2006; 24:681–691. [PubMed: 16824962]
22. Petridou N, Plenz D, Silva AC, Loew M, Bodurka J, Bandettini PA. Direct magnetic resonance detection of neuronal electrical activity. Proc Natl Acad Sci U S A. 2006; 103:16015–16020. [PubMed: 17038505]
23. Chu R, de Zwart JA, van Gelderen P, Fukunaga M, Kellman P, Holroyd T, Duyn JH. Hunting for neuronal currents: absence of rapid MRI signal changes during visual-evoked response. NeuroImage. 2004; 23:1059–1067. [PubMed: 15528106]
24. Parkes LM, de Lange FP, Fries P, Toni I, Norris DG. Inability to Directly Detect Magnetic Field Changes Associated With Neuronal Activity. Magn Reson Med. 2007; 57:411–416. [PubMed: 17260380]
25. Tang L, Avison MJ, Gatenby JC, Gore JC. Failure to direct detect magnetic field dephasing corresponding to ERP generation. Magn Reson Imaging. 2008; 26:484–489. [PubMed: 18180125]
26. Romani, GL. Fundamentals on neuromagnetism. In: Wiliamson, S., editor. Advances in biomagnetics. Plenum; New York: 1989. p. 33-46.
27. Wikswo, JP. Biomagnetic sources and their models. In: Wiliamson, S., editor. Advances in biomagnetics. Plenum; New York: 1989. p. 1-19.
28. Norris DG. High Field Human Imaging. J Magn Reson Imaging. 2003; 18:519–529. [PubMed: 14579394]
29. Allison T, McCarthy G, Wood CC, Williamson PD, Spencer DD. Human cortical potentials evoked by stimulation of the median nerve. II. Cytoarchitectonic areas generating long-latency activity. J Neurophysiol. 1989; 62:711–722. [PubMed: 2769355]
30. Allison T, McCarthy G, Wood CC, Darcey TM, Spencer DD, Williamson PD. Human cortical potentials evoked by stimulation of the median nerve. I. Cytoarchitectonic areas generating short-latency activity. J Neurophysiol. 1989; 62:694–710. [PubMed: 2769354]
31. Backes WH, Mess WH, van Kranen-Mastenbroek V, Reulen JP. Somatosensory cortex responses to median nerve stimulation: fMRI effects of current amplitude and selective attention. Clin Neurophysiol. 2000; 111:1738–1744. [PubMed: 11018487]
32. Schulz M, Chau W, Graham SJ, McIntosh AR, Ross B, Ishii R, Pantev C. An integrative MEG-fMRI study of the primary somatosensory cortex using cross-modal correspondence analysis. NeuroImage. 2004; 22:120–133. [PubMed: 15110002]

33. Kakigi R. Somatosensory evoked magnetic fields following median nerve stimulation. Neurosci Res. 1994; 20:165–174. [PubMed: 7808699]

34. Hagberg GE, Bianciardi M, Maraviglia B. Challenges for detection of neuronal currents by MRI. Magn Reson Imaging. 2006; 24:483–493. [PubMed: 16677955]

35. Hamalainen M, Hari R, Ilmoniemi RJ, Knutila J, Lounasmaa OV. Magnetoencephalography-theory, instrumentation, and applications to noninvasive studies of the working human brain. Rev Mod Phys. 1993; 65:413–497.

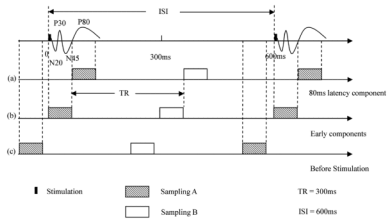

FIG. 1.

(a) The msMRI paradigm for detecting the 80 ms latency component. Data were acquired 50ms~110ms after stimulation onset (sampling A). (b) The msMRI paradigm for detecting the early components. Data were acquired 0ms~60ms after stimulation onset (sampling A). (c) Data were acquired (-100~-40ms), i.e., before stimuli were presented (sampling A). No msMRI effects were obtained in this scan. Sampling B is control image.

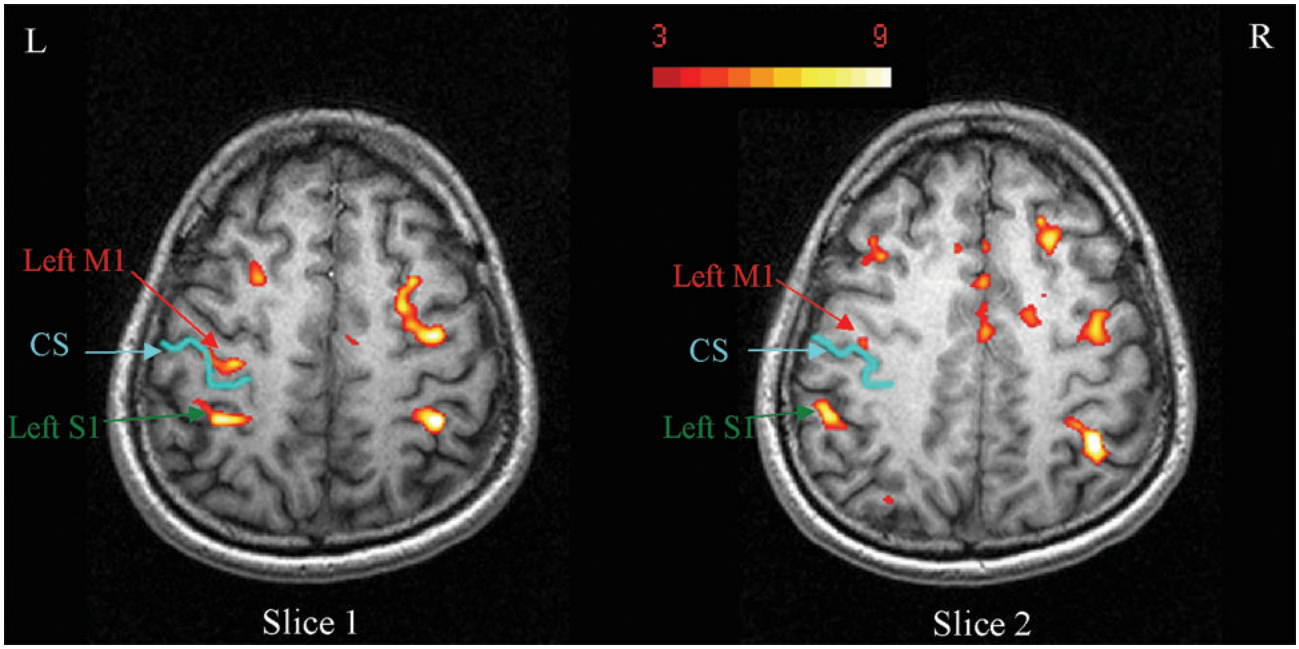

FIG. 2.

BOLD activation maps for two contiguous slices which cover S1 and M1 areas. Significant activation clusters were found in contralateral primary sensory cortex (S1), and primary motor cortex (M1).

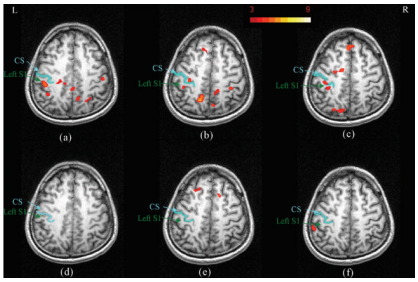

FIG. 3.

Figure 3a-3b shows msMRI activation maps of 80ms latency component for subject 1 on three different scanning days. The slice positions were manually selected to be as similar as possible. Activations in S1 were replicated. Figure 3d-3f shows the activation maps for the control scans in which no stimuli were applied. As expected, no activation was found in area S1.

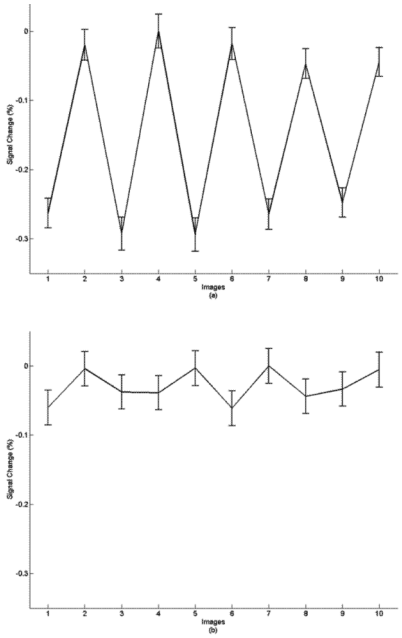

FIG. 4.

Time-course plots corresponding to the activated S1 area (a) and non-activated area (b) in 80ms latency effect scans. Odd numbers indicate stimulation On, even numbers represent the resting state. Each point on the time course represents an average of 120 images. The signal variance in activated S1 area was about 0.24% with good trial-by-trial consistency. The signal variance in the non-activated area is about 0.05%, and looks more random.

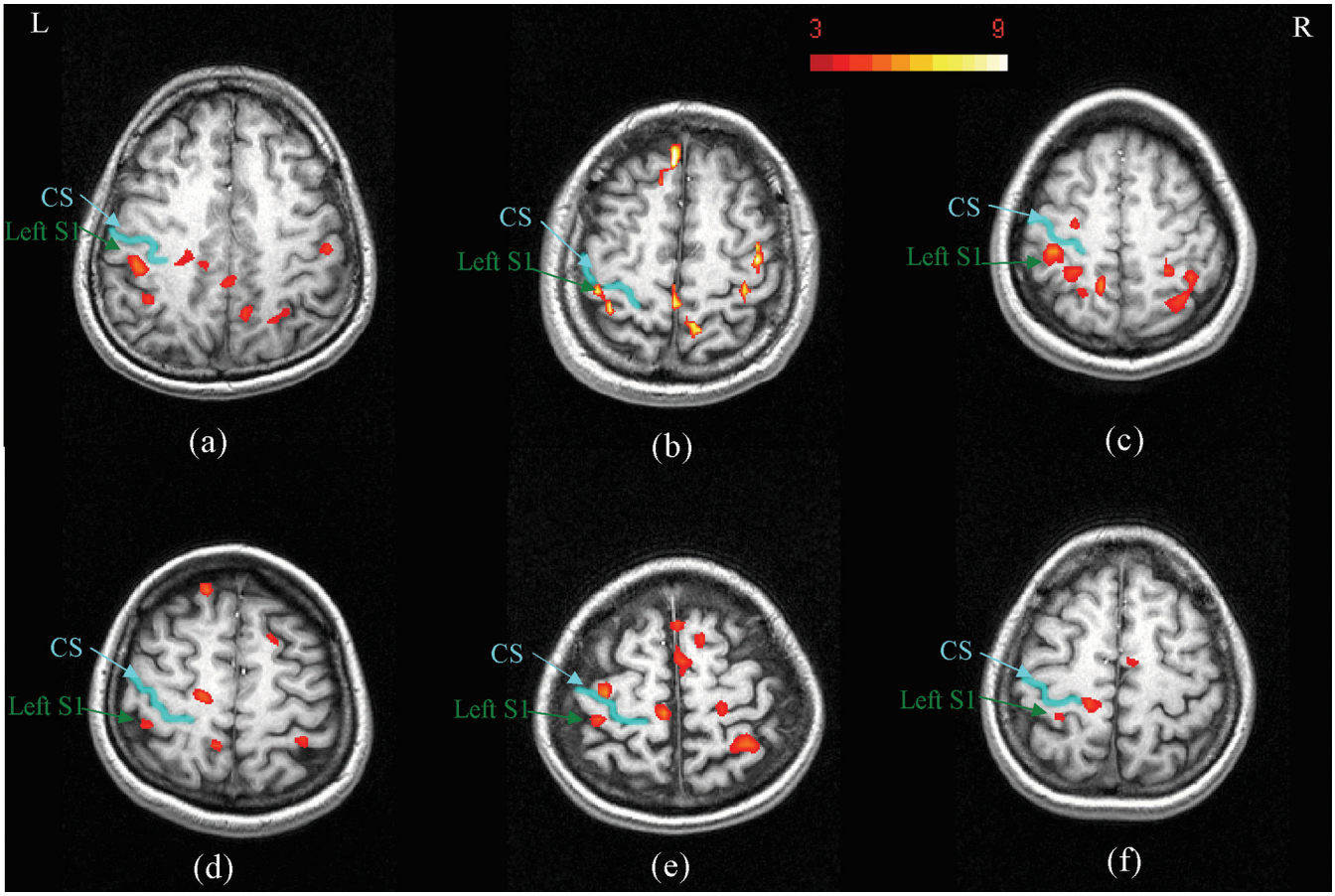

FIG. 5.
(a)-(f) are correspond to activation maps for subjects 1-6. All scans used an identical protocol. Activations in area S1 have good consistency across subjects, but activations in other areas (e.g. M1) have less consistency.

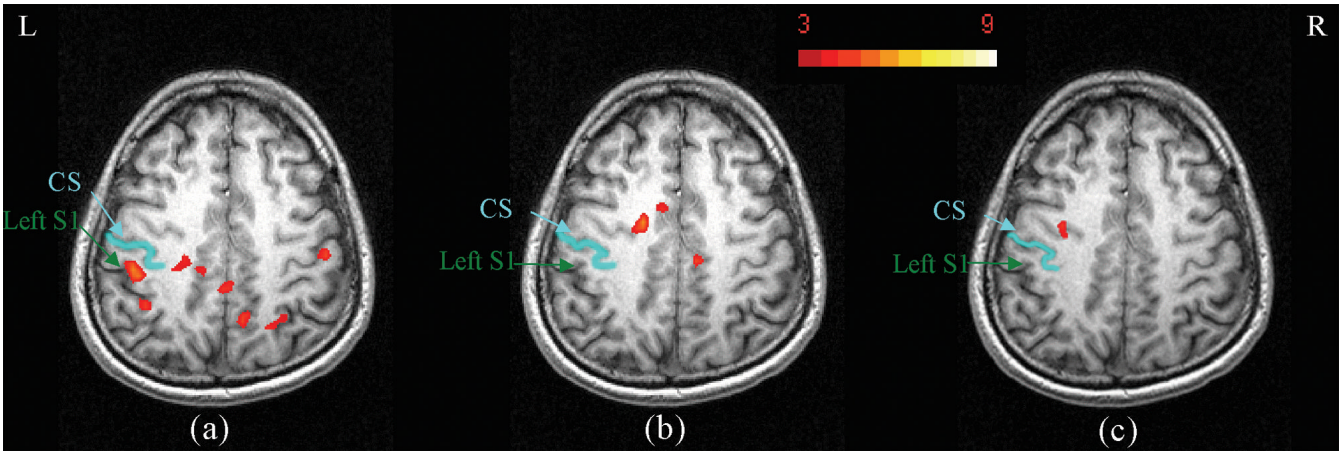

FIG. 6.

Activation maps demonstrating the timing effect. Figure 6a-6c shows the dephasing effects for the 80ms latency component, early components and the control scan acquired before stimulation. Significant activation was found in S1 area in figure 6a, but was not found in figure 6b or 6c. The absence in 6b is probably due to a cancellation effect as discussed in the text. The absence in 6c is expected because the stimulus had not been applied when the data were acquired.

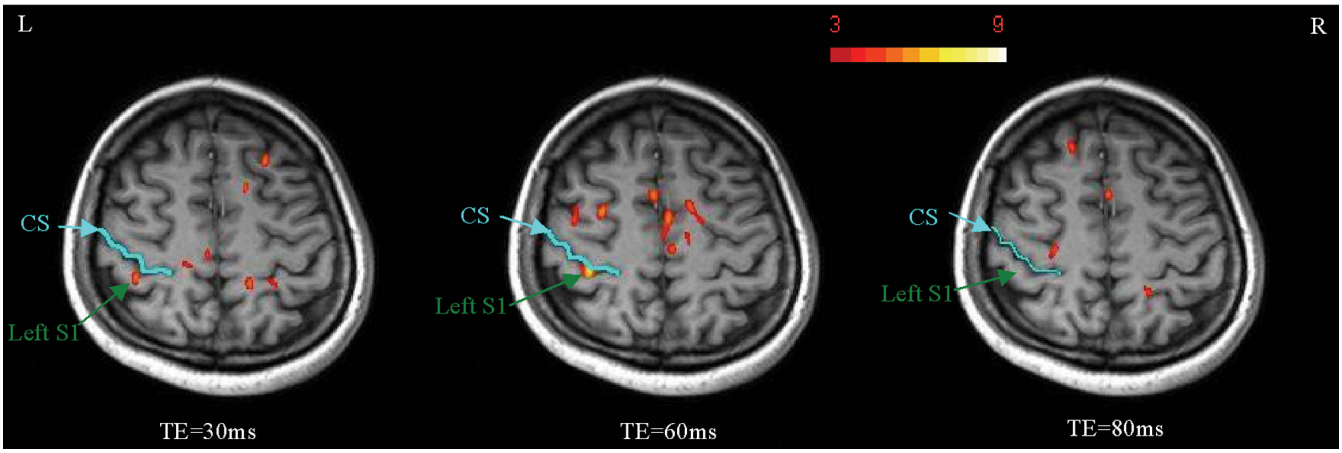

FIG. 7.

The activation maps for TE of 30 ms, 60 ms and 80 ms. Significant activations were found in S1 area for both TE of 30 ms and 60 ms. There was no activation in S1 area for TE of 80 ms. While the signal percentage change for TE of 80 ms was close to TE of 60 ms, the CNR for TE of 80 ms was only 57% of the CNR for TE of 60 ms.

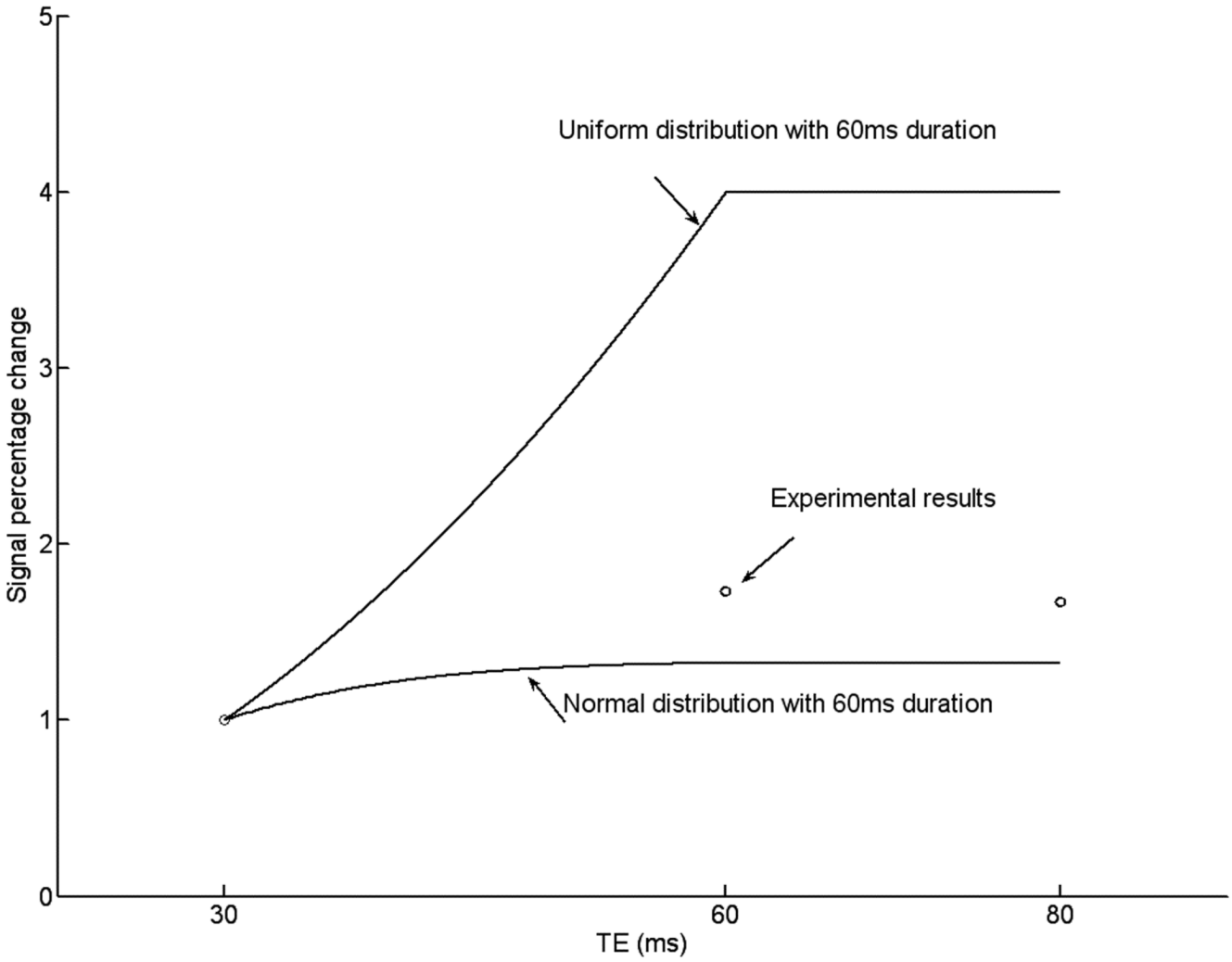

FIG. 8.

The signal percentage changes for different TEs and distributions. For the simulated data (solid line), a limited duration (60ms) of neuronal activity was assumed. No opposite neuronal magnetic field was considered. We assumed that the total number of neurons fired during the TE are same for both uniform and normal distributions. All data have been normalized to TE of 30 ms.. The TE was centered at P80 component (TE/2 was located at 80ms after stimulus).